Journal of Materials and Environmental Science
ISSN : 2028-2508
e-ISSN : 2737-890X
CODEN : JMESCN

J. Mater. Environ. Sci., 2025, Volume 16, Issue 8, Page 1426-1437

http://www.jmaterenvironsci.com

Inhibition of steel corrosion in oilfield acidizing environment using cashew nut shell liquid: Preliminary experimental and computational studies

Ekemini Ituen[1,2]*, Anyanime Etuk[2], Godwin Akpan[2], Innocent Afangide[2], Iniubong Umana[1,2], Solomon Shaibu[1,2], Udoinyang Inyang[3]

[1]*Computational Materials Science Group, TETFund Centre of Excellence in Computational Intelligence, University of Uyo, Uyo, Nigeria.*

[2]*Materials and Oilfield Chemistry Research Group, Department of Chemistry, University of Uyo, Uyo, Nigeria.*

[3]*Department of Data Science, Faculty of Computing, University of Uyo, Uyo, Nigeria*.

*Corresponding author: *ekeminiituen@uniuyo.edu.ng*

Received *25 April 2025,*
Revised *29 June 2025,*
Accepted *03 July 2025*

Keywords:
- ✓ *Adsorption*
- ✓ *Technical CNSL;*
- ✓ *Natural CNSL*
- ✓ *Density functional theory*
- ✓ *X80 steel*

Citation: Ituen, E., Etuk A., Akpan, G., Afangide, I., Unama, I., Shaibu, S., Inyang, U. (2025). Inhibition of steel corrosion in oilfield acidizing environment using cashew nut shell liquid: Preliminary experimental and computational studies. J. Mater. Environ. Sci., 16(8), 1426-1437

Abstract: During local processing of cashew, the shell is often discarded as waste after the nuts have been obtained by de-kernelling. From this shell, a dark-brown syrupy liquid was extracted in ethanol-water solution and heat-treated to obtain natural cashew nut shell liquid (n-CNSL) and technical cashew nut shell liquid (t-CNSL). Both n-CNSL and t-CNSL were evaluated as corrosion inhibitors in 5% hydrochloric acid solution at 30 oC to 80 oC using weight loss technique. Higher doses of n-CNSL and t-CNSL inhibited corrosion of X80 steel in the 5% HCl medium than lower doses indicating that inhibition efficiency was concentration dependent. Unlike many plant-based materials, the inhibition efficiency increased as temperature increased reaching maximum values at 60 oC. Although both n-CNSL and t-CNSL exhibited impressive inhibitive effects, the n-CNSL was more efficient than t-CNSL under same conditions. This was attributed to the multifunctional nature of anacardic acid, a phnolic compound that is more abundant in n-CNSL than cardanol and cardol which are also constituents of both liquids. Density functional theory computations conducted on the three phenolic compounds implicated carboxylic and hydroxyl groups as potential adsorption sites for electron donor and acceptor interactions with d-orbitals of iron. Results from this preliminary assessment has demonstrated that both n-CNSL and t-CNSL have the potentials for deployment as ingredients in oilfield corrosion inhibitor formulations.

1. Introduction

Acid, especially hydrochloric acid (HCl), is commonly used in the oilfield for cleaning, descaling and well stimulation procedures (Elayachy *et al.*, 2021; Finsgar and Jackson, 2014; Elayachy *et al.*, 2005). The concentration of the acid to be used depends on the purpose for its deployment. For cleaning and descaling operations, 1 M HCl is usually deployed whereas for acidizing procedures, high concentration ranging from 5 -15 % is used (Ituen *et al.*, 2021). This concentration of HCl is corrosive and the acid often attacks steel structural materials as well as pipework. Over time, this results in failure of materials, consequently leading to spills or other undesirable outcomes. Thus, the steel materials

need to be protected from corrosion to enhance its longevity, hence, corrosion inhibitors are often added to the acidic medium. Corrosion inhibitors (CIs) do not actually stop corrosion - they mainly retard the rate at which corrosion occurs (Zakeri *et al.*, 2022). It has been established that CIs achieve this by adsorbing on the steel surface and forming a thin layer that 'blankets' the surface from the aggressive acids stream (Alareeqi *et al.*, 2021; Ituen *et al.*, 2016). The adsorption is usually facilitated by some electron-rich moieties which such as hetero-rings, aromatic rings, multiple bonds, and some atoms such as O, N, P, S that may be present in the CI molecule (Elabbasy *et al.*, 2024; Zarrok *et al.*, 2012).

Among the various materials that have been tested as corrosion inhibitors are some non-biodegradable materials (which are considered to be environmentally unfriendly), or materials that are very expensive to purchase in large quantity or rigorous to synthesize in good quantity. This has shifted focus to CIs that can be derived from local materials (especially plant biomasses) because such would be cost effective, biodegradable, sustainable, renewable and eco-friendly (Alao *et al.*, 2023; El Azzouzi *et al.*, 2022; Lazrak *et al.*, 2021; El Faydy *et al.*, 2020). The choice of a local material for extraction and preparation of CIs is often influenced by the nature of the compounds present and the ease of extraction. In addition, while using the material for extracting CIs, ensuring that there is no competition with food is very essential. This makes utilization of agro-industrial by-products or agro-wastes and non-food plants of comparable advantage.

In this study, native cashew nut shell liquid (CNSL) is tested as corrosion inhibitor for X80 steel in 5 % HCl HCl. Although cashew is very abundant in Nigeria, there are a few reports on the use of the liquid for inhibiting corrosion (Achin and Myina, 2011; Enabulele *et al*, 2023; Fayomi *et al.*, 2021). In the few reports available, the cashew nuts used to extract the liquid were not obtained from Akwa Ibom state. In addition, the tests were conducted in low concentrations (1 M) of acid. For plants, the chemical composition varies depending on geographical location where the plant grows, soil type and species of the plant (Ghasemzadeh *et al*., 2018; Tursun, 2022). While the results for the efficiency of the CNSL grown in the reported parts of Nigeria looks impressive, the present study seeks to benchmark the one harvested in Uyo, Akwa Ibom state and also compare results.

Generally, cashew nut shell (CNS) has been reported to make up about 67% of cashew nut and contains 30 – 35% CNSL (Nyirenda *et al.*, 2021; Magaya *et al.*, 2019). The CNSL contains mainly cardanol (CD), anacardic acid (AA) and cardol (CL), all of which are phenolic compounds (Garkal and Bhande, 2014). The molecular structures of CD, AA and CL (Fig. 1) are related and contains aromatic ring, double bond and O atoms which may be considered as potential adsorption sites for corrosion inhibition.

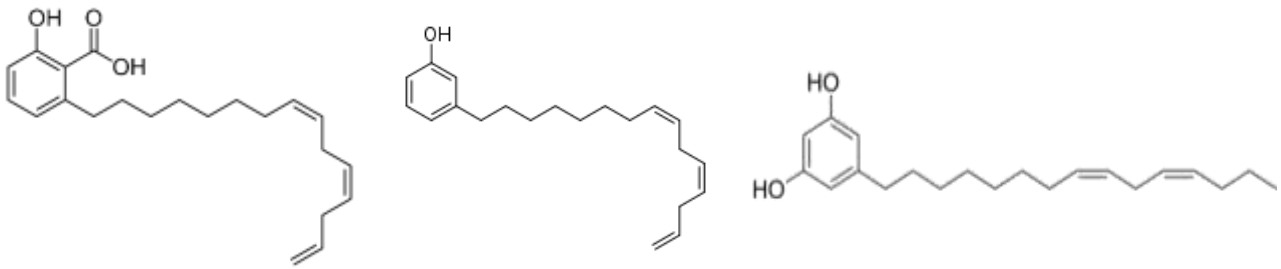

Anacardic acid Cardanol Cardol

Fig. 1. Molecular structures of the key phenolic compounds in CNSL.

Practically, there are two forms of CNSL, namely, natural (n-CNSL) and technical (t-CNSL) (Medeiros *et al*., 2020). Natural CNSL can be extracted from *Anacardium accidentale* at low temperature whereas t-CNSL is obtained through high temperature treatment. Preliminary assessment of the two treated forms by GC-MS and HPLC-MS reveals that n-CNSL contains 72 % anacardic acid, 5 % cardanol, 20 % cardol and 3 % 2-methylcardol whereas t-CNSL contains 1.5 % anacardic acid, 76 % cardanol, 18 % cardol and 4.5 % 2-methylcardol (Ike *et al*., 2021). The percentage of anacardic acid in technical CNSL is low because treatment at temperature above 140 ^{o}C decarboxylates anacardic acid to cardanol, leading to the increased percentage of cardanol in t-CNSL and reduced percentage of anacardic acid.

2. Materials and method

2.1 Preparation of CNSL

Mature cashew fruits were obtained from Cashew plantation behind Uyo Village Road in Uyo Local Government Area of Akwa Ibom state in Nigeria and conveyed to our laboratory. They were identified in the department of Botany and Ecological Science as *Anacardium occidentale*. The seeds were separated from the fruits, and then de-kernelled to separate the nuts from the extracted in water-ethanol (30:70) by maceration in glass jar following 72 hours soaking. This was followed by filtration and another 72 hours re-maceration to completely extract the bioactive compounds. The filtrate (CNSL) obtained were concentrated using DK420 water-bath. A portion of the filtrate was warmed at 50 - 70 ^{o}C to obtain n-CNSL whereas another portion of the filtrate was subjected to heat treatment at 140 ^{o}C to obtain t-CNSL. The liquids were stored in laboratory refrigerator for subsequent use.

2.2 Steel specimens

Corrosion test was conducted by deploying weight loss technique under total immersion imitating anaerobic condition. First, X80 steel coupons (4 cm x 5 cm) obtained from Shengxin Technology Co. Ltd, Xinyang, China, were abraded with various grades of SiC paper to near mirror surface finishing, degreased in absolute ethanol, cleaned according to ASTM G1-9022 procedures and stored in sealed water-proof bags in moisture-free dessicator. As quoted by the supplier, the chemical composition (w/w%) of the was: Si (0.065), Mn (1.58), P(0.011), S(0.003), Cu(0.01), Cr(0.022), Nb (0.057), V(0.005), Ti(0.024), B(0.006) with Fe constituting the balance.

2.3 Test solutions

Analytical grade (BDH) HCl supplied by Double Bond Chemicals, Uyo, Akwa Ibom State, Nigeria, was prepared into 5 % concentration to simulate oilfield scale wash fluid. About 10 mL of the CNSL was diluted in the 5 % HCl solution and made up to 1000 mL. This was repeated using 20 mL, 50 mL and 100 mL of CNSL each to make 1000 mL solution.

2.4 Corrosion test

Pre-cleaned steel coupons were weighed (w_o) and suspended in 100 mL beakers each containing different test solution, then the vessel was sealed using aluminium foil and placed in water bath maintained at 30 ^{o}C for 5 h (Ituen *et al*., 2021). Thereafter, the vessels were retrieved from water bath, coupons were retrieved, cleaned using ASTM G1-90 standard, rinsed in acetone, allowed to air-

dry and re-weighed (w_1). The test solutions included the 5 % HCl solution as blank, and with addition of 10 Ml, 20 mL, 50 mL and 100 mL of CNSL. The immersion procedure was also repeated at 40, 50, 60 and 80 ^{o}C. The weight loss (ΔW) of each coupon was recorded and used to calculate the corrosion rate (CR (mmpy)) and inhibition efficiency (%E) using Eqs. 1 and 2, respectively (Ladan *et al.*, 2025; Bouklah *et al.*, 2006).

$$CR = \frac{87.6\,(w_1 - w_0)}{\rho A t} \quad (1)$$

$$\%E = 100\left(\frac{CR_a - CR_i}{CR_a}\right) \quad (2)$$

where CR_a is the corrosion rate in the blank solution with only 5 % HCl and CR_i is the corrosion rate in the presence of the different amounts of CNSL, A is the average surface area of the steel coupon and t is the time of immersion.

2.5 Computational technique

The computations were carried out with the help of Material Studio software, BIOVIA, Dassault Systemes, United States (2017). The molecular structures of AA, CD and CL were built using the 3D Atomistic tool of the software. The geometry of each molecule was optimized using Forcite tool to arrive at the most stable configuration. Electronic structure modelling was performed using the Dmol^3 module of the software with the Becke–three-Lee–Yang–Parr (B3LYP) functional, using the double numeric with polarization (DNP) basis set (Shehu and Usman, 2023). The plots and energies of the molecular orbitals (MO), namely, the highest occupied MO (E_{HOMO}) and the lowest unoccupied MO (E_{LUMO}) were obtained. Some molecular reactivity indices such as LUMO-HOMO energy gap (ΔE), ionization energy (IE) and electron affinity (EA) were calculated by applying Eqs. 3 – 5 (Ituen *et al.*, 2019):

$$\Delta E = E_{LUMO} - E_{HOMO} \quad 3$$

$$IE = -E_{HOMO} \quad 4$$

$$EA = -E_{LUMO} \quad 5$$

Similarly, electronegativity (χ), global hardness (η) and global softness (σ) were be calculated using Eqs. 6 – 8 (Ituen *et al.*, 2019):

$$\chi = \frac{1}{2}(IE + EA) \quad 6$$

$$\eta = \frac{1}{2}(IE - EA) \quad 7$$

$$\sigma = \frac{1}{\eta} \quad 8$$

From the optimized structure, Fukui electrophilic and nucleophilic functions were calculated by Mulliken population analysis. Also, to screen for possible adsorption sites on the molecules, the Mulliken atomic charge distribution was calculated.

3. Results and discussion

3.1 Corrosion inhibition

The corrosion rate and inhibition efficiency data obtained at the different temperatures studied are displayed in **Table 1 and 2** for n-CNSL and t-CNSL respectively. As may be observed from the tables, corrosion rate, just like typical rates of chemical reactions, increases as temperature increases. At 30 ^{o}C, the rate at which 5% HCl corrodes the steel surface was 2.733 mmpy but this rate increased to 5.628 mmpy at 40 ^{o}C and upto 37.130 mmpy at 80 ^{o}C. On addition of CNSL, corrosion rate reduced drastically and the extent of reduction was dose-dependent. The higher the dose of CNSL in the test solution, the lower the corrosion rate. This indicates that a CNSL actually inhibits the corrosion of the steel specimens in the aggressive solution. The extent of inhibition of the corrosion (measured in terms of efficiency) can be observed to increase as dose of CNSL increases and also as temperature increases.

Table 1. Corrosion rate and inhibition efficiency of different loading of n-CNSL at 30 – 80 ^{o}C

n-CNSL	**30 ^{o}C**		**40 ^{o}C**		**50 ^{o}C**		**60 ^{o}C**		**80 ^{o}C**	
dose (mL/L)	CR	$\%E$	CR	$\%E$	CR	$\%E$	CR	$\%E$	CR	$\%E$
0	2.733	-	5.628	-	11.281	-	19.841	-	37.130	-
10	0.812	70.3	1.525	72.9	2.786	75.3	4.702	76.3	9.987	73.1
20	0.765	71.9	1.452	74.2	2.459	78.2	4.107	79.5	9.728	75.3
50	0.694	74.6	1.216	78.4	1.951	82.7	3.274	83.5	6.646	82.1
100	0.593	78.3	1.092	80.6	1.703	84.9	2.817	85.7	5.718	84.6

Table 2. Corrosion rate and inhibition efficiency of different loading of n-CNSL at 30 – 80 ^{o}C

Amount of	**30 ^{o}C**		**40 ^{o}C**		**50 ^{o}C**		**60 ^{o}C**		**80 ^{o}C**	
t-CNSL	CR	$\%E$	CR	$\%E$	CR	$\%E$	CR	$\%E$	CR	$\%E$
0 mL	2.733	-	5.628	-	11.281	-	19.841	-	37.130	-
10 mL	0.987	63.9	1.981	64.8	3.824	66.1	6.885	65.3	15.669	57.8
20 mL	0.896	67.2	1.722	69.4	3,226	71.4	5.873	70.4	14.258	61.6
50 mL	0.853	68.8	1.654	70.6	3.023	73.2	5.734	71.1	12.550	66.2
100 mL	0.809	70.4	1.480	73.7	2.471	78.1	4.702	76.3	11.213	69.8

It has been established that plant extracts and organic molecules inhibit corrosion by adsorption mechanism. That is, the organic compounds in the extract drift from the bulk phase to the steel surface and become adsorbed on the surface. The adsorptive binding of the compounds to the steel surface may be driven by physical forces such as electrostatic interactions, hydrogen binding interactions, or van der walls interactions (physical adsorption) or may be driven by chemical interactive forces such as

actual chemical bonding forces (chemical adsorption). The type of driving force and mechanism may be predicted from the trend which inhibition efficiency varies with temperature. For physical adsorption mechanism, the amount adsorbed decreases as temperature increases, whereas for chemical adsorption mechanism, the amount adsorbed increases as temperature increases. From the trend of results, it can be inferred that the adsorption of organic compounds in CNSL on the steel surface occurs via chemical adsorption mechanism.

A comparison of the inhibition efficiency values in **Table 1** with those in **Table 2** reveals that n-CNSL is more efficient in inhibiting the corrosion than t-CNSL, at all concentrations and temperatures. It has been reported that n-CNSL, which is prepared at low temperature, contains mainly AA (71 - 82%), CL (13 – 20 %)) and CD (1 – 9%). On the other hand, t-CNSL, which is prepared through heating at higher temperature, contains higher CD (67 – 94%) and lower AA (1 – 2%)) and CL (3 – 18%) (Rojtman *et al*., 2024). A close observation of the functional groups in these phenolic compounds reveal that n-CNSL would contain more –COOH groups than t-CNSL. This could be responsible for the observed higher efficiency of n-CNSL over t-CNSL. However, further insights into this were obtained by quantitative structure-reactivity assessment using quantum chemical studies.

3.2 Geometry optimization

The optimized structures of AA, CD and CL obtained are shown in **Fig. 2.** The energies and convergence obtained on optimizationare depicted in Fig. 3. The downward trend that eventually levels out near the threshold indicates successful convergence. The structures depict the lowest energy conformations of anacardic acid, cardanol and cardol with total energy (kcal/mol) of -60.167708 (-251.4 kJ/mol), -38.709026 (-161 kJ/mol) and -61.903782 (-258 kJ/mol), respectively. This energy value is expected to be the minimum energy for the most stable configuration of each of the molecules. The shapes of the optimized geometries seem to be planar, and it has been reported that planar geometries enhance better adsorption and corrosion inhibition (Singh *et al*., 2019) because it enhances coverage of a large area of the substrate surface.this observation provided prior insight that the molecules could likely adsorb efficiently on steel surface.

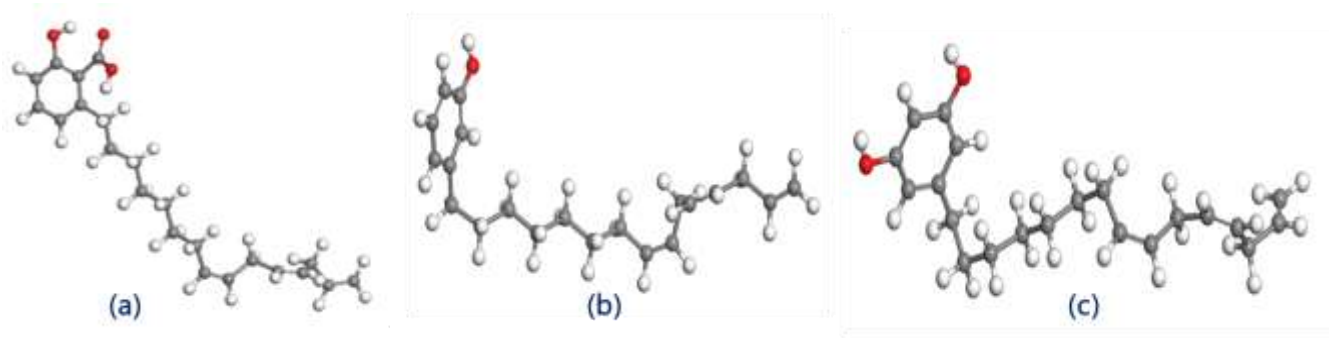

Fig. 2. Optimized structures of (a) anacardic acid (b) cardanol and (c) cardol as determined by DFT/DNP [Grey (carbon), white (hydrogen), red (oxygen)].

The values of the computed total energies indicate that cardol exhibits the most thermodynamically stable conformation among the three, with the lowest total energy (−258.2 kJ/mol), closely followed by anacardic acid (−251.4 kJ/mol). Cardanol, with a significantly higher energy

(−161.9 kJ/mol), appears to be the least stable of the trio with respect to its optimized geometry. This difference in stability may be attributed to the number and position of hydroxyl functional groups and the degree of conjugation across the molecular frameworks. Cardol, bearing two hydroxyl groups directly attached to the aromatic ring, is likely stabilized via intra-molecular hydrogen bonding and resonance delocalization, whereas cardanol possesses a single hydroxyl group, reducing such stabilizing interactions. These findings provide foundational insight into the intrinsic stability of these compounds and can be instrumental in understanding their reactivity profiles, binding affinities, and their adsorption characteristics.

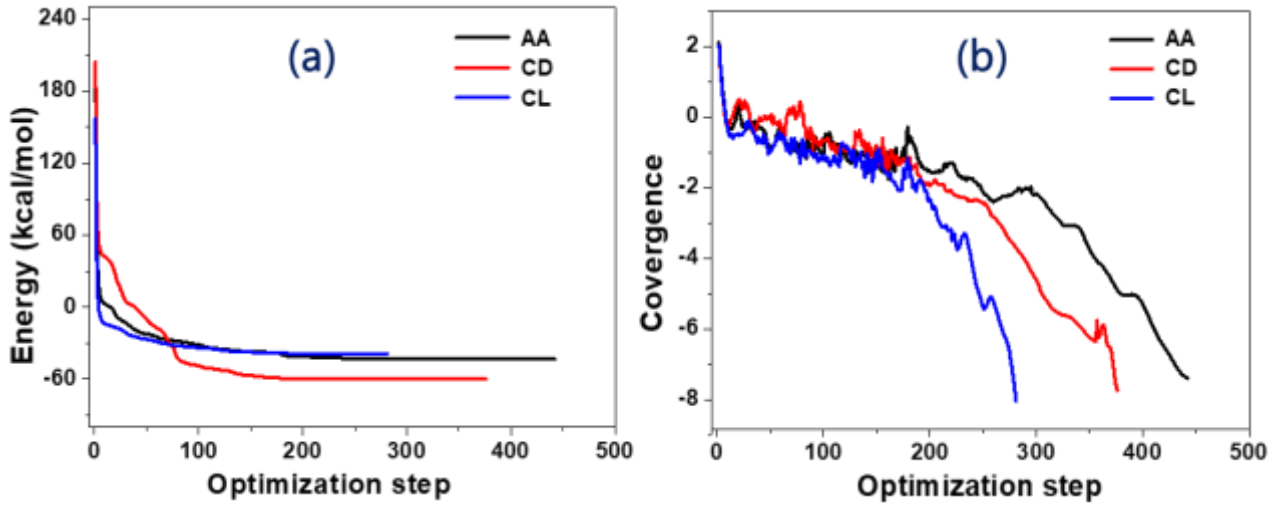

Fig. 3. (a) Energy plots and (b) convergence from geometry optimization of anacardic acid, cardanol and cardol in CNSL.

3.3 HOMO and LUMO orbitals and energies

The HOMO and LUMO energies are crucial pointers to molecular reactivity and interaction with metallic surfaces. Results of the orbital energies are shown in **Table 1** whereas the plots of the orbitals are shown in Fig. 4. and Fig. 5. Cardol showed the highest HOMO energy (-5.517 eV) among the studied compounds, indicating that it possesses the strongest electron-donating capability toward the unoccupied d-orbitals of iron. In contrast, anacardic acid and cardanol exhibited lower HOMO energies (-5.682 eV and -6.118 eV, respectively), indicating comparatively reduced abilities to donate electrons.

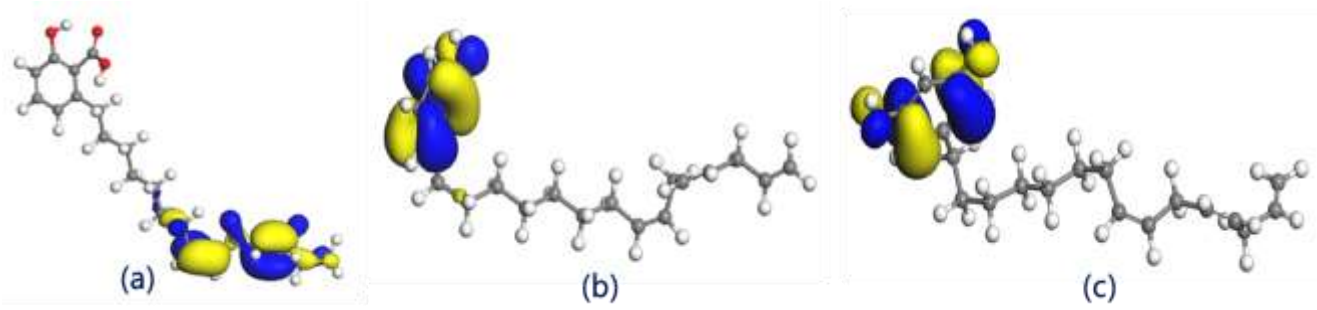

Fig. 4. Highest occupied MO (HOMO) plot of (a) Anacardic acid (b) Cardanol and © cardol using DFT/DNP.

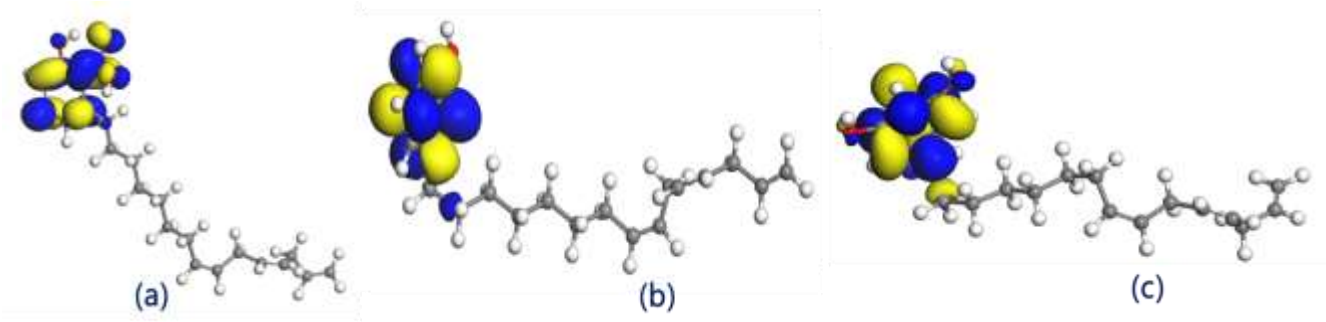

Fig. 5. Lowest unoccupied MO (LUMO) plot of (a) Anacardic acid (b) Cardanol and (c) Cardol using DFT/DNP.

The high HOMO level of CL implies that it can strongly adsorb onto the metal surface via donation of its lone pair electrons, especially from electronegative atoms such as oxygen. The LUMO energies, which reflect the ability to accept electrons, were lowest for CD (-1.148 eV), followed by AA (0.221 eV) then CL (0.347 eV). A lower LUMO energy implies a stronger ability to accept back-donated electrons from the iron surface, enhancing chemisorption and surface passivation. Thus, the HOMO-LUMO analysis reveals that CL would exhibit the most favourable orbital interactions with steel substrate.

3.4 Energy Gap and molecular reactivity

The magnitude of the energy gap (ΔE) is considered to relate inversely with the chemical reactivity of a molecule. Smaller energy gaps facilitate better charge transfer between the inhibitor and the metal surface. As may be observed from results, CD exhibits the smallest energy gap (4.970 eV) compared to AA (5.903 eV) and CL (5.864 eV). Thus, it can be implied that CD having the lowest ΔE would be enhance better electron transfer and hence higher inhibition capacity (Gebremeskel *et al*., 2024).

3.5 Potential adsorption sites

The Fukui functions obtained provided further insight into the local reactivity of the molecules studied. For AA, the carboxylic acid group and phenolic oxygen are sites showing the highest values of nucleophilic and electrophilic Fukui functions, identifying them as the principal sites for metal interaction. As may be observed from **Fig. 4** and **Fig. 5**, the aromatic system also contributes to the delocalization of electron density, enhancing adsorption which may occur through π-back-bonding mechanisms. In CD and CL, the phenolic hydroxyl groups also remain the potential active centers, however, the absence of additional polar functional groups like the carboxylic acid reduces the number of potential bonding sites. Consequently, AA could exhibit from both electrostatic interactions and chemical adsorption, owing to the multifunctional nature of its structure (Kamarul Baharin *et al.*, 2025; Haldhar *et al.*, 2021; Karzazi *et al*., 2016).

3.6 Comparative inhibitory potential and experimental results

By integrating all the quantum descriptors, the higher HOMO energy and the lower ΔE, it can be predicted that CD would exhibit better interaction with the steel surface and hence t-CNSL which is richer in CD would afford higher inhibition efficiency. However, experimental results show otherwise. Instead, n-CNSL which is richer in AA afforded higher inhibition efficiency. This could be due to the multifunctional nature of AA compared to CD and CL. The presence of both –OH and –

COOH group in addition to the aromatic ring may have conveyed higher adsorption and affinity on AA towards steel surface, resulting in higher inhibition efficiency. While all three major compounds in CNSL share a phenolic backbone, the presence of additional electron-donating and polar groups in anacardic acid significantly enhances the performance of n-CNSL. We can also introduce the intermolecular synergistic effect of the various components to ensure protect metal surface against aggressive ions (Ameh *et al*., 2025; Abakedi & Anweting, 2024; Lrhoul *et al*., 2023; Salim *et al*., 2022)

Conclusion

Natural and technical cashew nut shell liquids have been prepared from the syrupy liquid extracted from cashew nut shell by heat treatment. The liquids have been assessed as corrosion inhibitors for X80 steel in 5% HCl solution. Both n-CNSL and t-CNSL inhibits the corrosion process but n-CNSL afforded higher efficiencies than t-CNSL. Inhibition efficiency increases with increase in CNLS dose and increase in temperature. Inhibitive effect is due to both electrostatic interaction and chemisorption of active molecules, namely, anacardic acid, cardanol and cardol on the steel surface. Density functional theory calculations provides insights that adsorption may be facilitated by –COOH and –OH functional groups. From findings, it was concluded that both n-CNSL and t-CNSL are potential ingredients for deployment in formulating corrosion inhibitors for low concentration acidizing media.

Acknowledgements: The authors are grateful for the Institutional Based Research (IBR) initiative, funded by the Tertiary Education Trust Fund (TETFund) which provided funding for this work through the 2023 IBR grant, University of Uyo, Uyo, Nigeira.

References

Abakedi O. U, Anweting I. B. (2024). Eco–friendly impact of orange (Citrus sinensis) seed extract as corrosion inhibitor for aluminium in 2 M HCl solution, *J. Mater. Environ. Sci.*, 15(3), 441-451

Achi, S. S., Myina, O. M. (2011). Preliminary investigation of Kaduna-Grown cashew nutshell liquid as a natural precursor for dyestuffs, pigments and binders for leather finishing. *Nig. J. Chem. Res.* 16, 9-14.

Alao A.O., Popoola A.P., Dada M.O. and Sanni O. (2023) Utilization of green inhibitors as a sustainable corrosion control method for steel in petrochemical industries: A review. *Front. Energy Res.* 10, 1063315. doi: 10.3389/fenrg.2022.1063315

Alareeqi, S., Bahamon, D., Nogueira, R. P., Vega, L. F. (2021). Understanding the relationship between the structural properties of three corrosion inhibitors and their surface protectiveness ability in different environments. *Appl. Surf. Sci.* 542, 148600.

Ameh E. M., Ekwoba L., Ocheme G. W., Oteno F., Umar A. Y., Esseoghene E. L. (2025) Corrosion Inhibition Study Ethanolic Extract of Neem Leaves (Azadirachta indica) on Zinc metal in 0.1 M HCl and 0.1 M NaOH, *J. Mater. Environ. Sci.*, 16(2), 341-353

Bouklah M., Ouassini K., Hammouti B., El Idrissi A. (2006), Corrosion inhibition of steel in sulphuric acid by pyrrolidine derivatives, *Appl. Surf. Sci.*, 252 (6), 2178-2185, https://doi.org/10.1016/j.apsusc.2005.03.177

Cheng, H. N., Furtado, R. F., Biswas, A., *et al*. (2022). Chemical modifications and applications of cashew byproducts-A selective review. *ACS Food Sci. Technol.* 3(4), 546-552.

Elabbasy, H. M., Toghan, A., Gadow, H. S. (2024). Cysteine as an eco-friendly anticorrosion inhibitor for mild steel in various acidic solutions: electrochemical, adsorption, surface analysis, and quantum chemical calculations. ACS Omega, 9(11), 13391-13411.

Elayyachy M., Elkodadi M., Aouniti A., Ramdani A., Hammouti B., Malek F., Elidrissi A. (2005), New bipyrazole derivatives as corrosion inhibitors for steel in hydrochloric acid solutions, *Mat. Chem. Phys.* 93(2-3), 281-285, https://doi.org/10.1016/j.matchemphys.2005.03.059

El Azzouzi M., Azzaoui K., Warad I., Hammouti B., *et al*. (2022), Moroccan, Mauritania, and Senegalese gum Arabic variants as green corrosion inhibitors for mild steel in HCl: Weight loss, Electrochemical, AFM and XPS studies, *Journal of Molecular Liquids*, 347, 118354, https://doi.org/10.1016/j.molliq.2021.118354

El Faydy M., Benhiba F., Berisha A., Kerroum Y., Jama C., *et al*. (2020) An experimental-coupled empirical investigation on the corrosion inhibitory action of 7-alkyl-8-Hydroxyquinolines on C35E steel in HCl electrolyte, *Journal of Molecular Liquids*, 317, 113973

Enabulele, D. O., Bamigboye, G. O., Solomon, M. M., Durodola, B. (2023). Exploration of the corrosion inhibition potential of cashew nutshell on thermo-mechanically treated steel in seawater. *Arab. J. Sci. Eng.* 48(1), 223-237.

Fan B., Zhao X., Liu Z., Xiang Y., Zheng X. (2022), Inter-component synergetic corrosion inhibition mechanism of Passiflora edulia Sims shell extract for mild steel in pickling solution: Experimental, DFT and reactive dynamics investigations, *Sustainable Chemistry and Pharmacy*, 29, 100821, ISSN 2352-5541, https://doi.org/10.1016/j.scp.2022.100821

Fayomi, O. M., Ike, D. C., Iorhemba, M. A., Ameh, O. M., Ihegwuagu, N. E., Kalu, R. C. (2021). Investigation on the corrosion inhibiting property of modified cashew nutshell liquid. *Int. J. Corros. Scale Inhib.* 10(3), 1307-1322.

Finšgar, M., Jackson, J. (2014). Application of corrosion inhibitors for steels in acidic media for the oil and gas industry: A review. *Corros. Sci. 86*, 17- 41.

Garkal, D. J., Bhande, R. S. (2014). Review on Extraction and Isolation of Cashew Nut Sh Ell Liquid. *Int. J. Innov. Eng. Res. Technol.* 1(1), 1-8.

Gebremeskel, H. M., Welearegay, M. A., Nadew, T. T. (2024). Computational Investigation of Corrosion Inhibition Properties of Hydrazine and Its Derived Molecules for Mild Steel. *Quantum Eng.* 2024(1), 5343086.

Ghasemzadeh, A., Jaafar, H. Z., Bukhori, M. F. M., Rahmat, M. H., Rahmat, A. (2018). Assessment and comparison of phytochemical constituents and biological activities of bitter bean (*Parkia speciosa Hassk*.) collected from different locations in Malaysia. *Chem. Cent. J.* 12, 1-9.

Haldhar, R., Prasad, D., Kamboj, D. *et al.* (2021). Corrosion inhibition, surface adsorption and computational studies of Momordica charantia extract: a sustainable and green approach. *SN Appl. Sci.* 3, 25, https://doi.org/10.1007/s42452-020-04079-x

Ike, D. C., Ibezim-Ezeani, M. U., Akaranta, O. (2021). Cashew nutshell liquid and its derivatives in oil field applications: an update. *Green Chem. Let. Rev.* 14(4), 620-633.

Ituen, E., Akaranta, O., James, A. (2016). Green anticorrosive oilfield chemicals from 5-hydroxytryptophan and synergistic additives for X80 steel surface protection in acidic well treatment fluids. *J. Mol. Liq*. 224, 408-419.

Ituen, E., Mkpenie, V., Ekemini, E. (2019). Corrosion inhibition of X80 steel in simulated acid wash solution using glutathione and its blends: Experimental and theoretical studies. *Coll. Surf. A: Physicochem. Eng. Asp*. 578, 123597.

Ituen, E., Singh, A., Yuanhua, L., Akaranta, O. (2021). Biomass-mediated synthesis of silver nanoparticles composite and application as green corrosion inhibitor in oilfield acidic cleaning fluid. *Clean. Eng. Technol.* 3, 100119.

Kamarul Baharin N.A.N., Sheikh Mohd Ghazali S.M.I.S., *et al.* Fazira Ilyana Abdul Razak, Siti Syaida Sirat, Tajuddin A.M., Kamarudin S.R.M., Dzulkifli N.N. (2025) Hirshfeld, Surface Analysis, DFT and Corrosion Inhibition Mechanism of Vanillin 4-ethylthiosemi carbazone on the Mild Steel in 1M HCl, *Mor. J. Chem.*, 13(1), 80-105, https://doi.org/%2010.48317/IMIST.PRSM/morjchem-v13i1.50111

Karzazi, Y., Belghiti, M. E., El-Hajjaji, F., Boudra, S., Hammouti, B. (2016). Density functional theory modeling and Monte Carlo simulation assessment of inhibition performance of two quinoxaline derivatives for steel corrosion. *J. Mater. Environ. Sci*., 7(11), 4011-4023.

Ladan, M., Ayuba, A. M., Zakariyya, D. (2025). Evaluation of Corrosion Inhibition Potential of Schiff Bases Derived from 2-Hydroxybenzaldehyde on Mild Steel in 1M HCl Solution. *J. Mater. Environ. Sci., 16* (2), 304, 319.

Lazrak J., Assiri El H., Arrousse N., El-Hajjaji F. *et al*. (2021). Origanum compactum essential oil as a green inhibitor for mild steel in 1 M hydrochloric acid solution: Experimental and Monte Carlo simulation studies, *Materials Today: Proceedings*, 45(8), 7486-7493; https://doi.org/10.1016/j.matpr.2021.02.233

Lrhoul H., Sekkal H. & Hammouti B. (2023) Natural Plants as Corrosion Inhibitors: Thermodynamic's restrictions, *Mor. J. Chem.*, 14(3), 689-698, https://doi.org/10.48317/IMIST.PRSM/morjchem-v11i3.40144

Medeiros, M. C., dos Santos, E. V., Martinez-Huitle, C. A., Fajardo, A. S., Castro, S. S. (2020). Obtaining high-added value products from the technical cashew-nut shell liquid using electrochemical oxidation with BDD anodes. *Sep. Purif. Technol*. 250, 117099.

Merimi I., Aslam R., Hammouti B., Szumiata T., *et al*. (2021), Adsorption and inhibition mechanism of (Z)-4-((4-methoxybenzylidene)amino)-5-methyl-2,4-dihydro-3H-1,2,4-triazole-3-thione on carbon steel corrosion in HCl: Experimental and theoretical insights, *Journal of Molecular Structure,* 1231, 129901 https://doi.org/10.1016/j.molstruc.2021.129901

Mgaya, J., Shombe G.B., Masikane S.C., *et al.* (2019). Cashew nut shell: A potential bio-resource for the production of bio-sourced chemicals, materials and fuels. *Green Chem.* 21, 1186–1201, https://doi.org/10.1039/C8GC02972E

Nyirenda, J., Zombe K., Kalaba G. *et al.* (2021). Exhaustive valorization of cashew nut shell waste as a potential bioresource material. *Sci Rep* 11, 11986, https://doi.org/10.1038/s41598-021-91571-y

Rojtman, E., Denis, M., Sirvent, C., Lapinte, V., Caillol, S., Briou, B. (2024). Polyols from Cashew Nutshell Liquid (CNSL), corner-stone building blocks for cutting edge biobased additives and polymers. *Polym. Chem.* 15, 4375-4415,

Salim R., Azzaoui K., Loukili E.H., Ech-chihbi E. (2022) Green corrosion inhibitors of carbon steel in acid medium: Plant extracts, *J. Appl. Sci. Envir. Stud.* 5(2), 75-86, https://doi.org/10.48393/IMIST.PRSM/jases-v5i2.45594

Shehu, U., Usman, B. (2023). Corrosion Inhibition of Iron Using Silicate Base Molecules: A Computational Study. *Adv. J. Chem. Sect. A.* 6, 334.

Singh, A., Ansari, K. R., Quraishi, M. A., Lin, Y. (2019). Investigation of corrosion inhibitors adsorption on metals using density functional theory and molecular dynamics simulation. In Corrosion Inhibitors. *IntechOpen*. DOI: 10.5772/intechopen.84126

Tursun, A. O. (2022). Impact of soil types on chemical composition of essential oil of purple basil. *Saudi J. Biol. Sci.* 29(7), 103314.

Zakeri, A., Bahmani, E., Aghdam, A. S. R. (2022). Plant extracts as sustainable and green corrosion inhibitors for protection of ferrous metals in corrosive media: A mini review. *Corros. Comm.* 5, 25-38.

Zarrok, H., Oudda, H., El Midaoui, A. *et al.* (2012). Some new bipyrazole derivatives as corrosion inhibitors for C38 steel in acidic medium. *Res. Chem. Intermed.*, 38, 2051–2063, https://doi.org/10.1007/s11164-012-0525-x